PHYSICAL REVIEW B **80**, 220405(R) (2009)

Model for frustrated spin-orbital chains as applied to CaV_2O_4

Gia-Wei Chern and Natalia Perkins
Department of Physics, University of Wisconsin, Madison, Wisconsin 53706, USA
(Received 28 July 2009; published 10 December 2009)

Motivated by recent interest in quasi-one-dimensional compound CaV_2O_4, we study the ground states of a spin-orbital chain characterized by an Ising-like orbital Hamiltonian and frustrated interactions between $S=1$ spins. The on-site spin-orbit interaction and the Jahn-Teller effect compete with intersite superexchange leading to a rich phase diagram in which an antiferro-orbital phase is separated from the orbital paramagnet by a continuous Ising transition. Two distinct spin liquids depending on the underlying orbital order are found in the limit of small spin-orbit coupling. In the opposite limit, the zigzag chain behaves as a spin-2 chain with Ising anisotropy. The implications for CaV_2O_4 are discussed.

DOI: 10.1103/PhysRevB.80.220405 PACS number(s): 75.10.−b, 71.10.−w

Orbital degrees of freedom have been shown to play an important role in understanding the electronic and magnetic properties of transition metal oxides.[1] This is particularly so for frustrated magnets with partially filled orbitals. A well-studied case is vanadium spinels AV_2O_4 where the A-site sublattice is occupied by divalent ions such as Zn^{2+} or Mn^{2+}.[2,3] The magnetic V^{3+} ions in spinel form a *pyrochlore* lattice. It is known that geometrical frustration of classical spins on such a lattice precludes simple Néel ordering and gives rise to a highly degenerate ground state. Orbital ordering in these compounds partially relieves the frustration by creating disparities in nearest-neighbor exchange constant, hence setting the stage for magnetic ordering at lower temperatures.[4,5]

In this Rapid Communication, we investigate the physics of frustrated vanadium chains in which the interplay of geometrical frustration, spin-orbital couplings, Jahn-Teller (JT) effect, and enhanced quantum fluctuations leads to a rich phase diagram. Our work is partly motivated by an attempt to understand another vanadium compound CaV_2O_4, which at room temperature crystallizes in the orthorhombic calcium-ferrite structure (space group *Pnam*).[6–10] Contrary to its spinel cousins, V^{3+} ions in CaV_2O_4 are arranged in zigzag chains of edge-sharing VO_6 octahedra (Fig. 1). Antiferromagnetic interaction on zigzag chains consisting of triangular loops is subject to geometrical frustration as well. The rather weak and frustrated interchain couplings make the vanadium chains quasi-one-dimensional (quasi-1D) systems susceptible to quantum fluctuations. Couplings of vanadium orbitals to spins and phonons add yet another dimension to the intriguing physics of zigzag chains.

In CaV_2O_4, the zigzag geometry results in a spin-1 chain with comparable nearest and next-nearest-neighbor interactions. Combined with the observation that the $3d^2$ configuration of V^{3+} ions tend to have an easy-plane anisotropy,[10] the quasi-1D compound CaV_2O_4 has been a favorable candidate for the long-sought chiral spin liquid where a long-range chiral order coexists with algebraically decaying spin correlations.[10,11] However, as first pointed out by Pieper *et al.*,[8] orbital degeneracy in this compound drastically changes the above picture. Since the t_{2g} levels are split into a singlet and a doublet due to a flattened VO_6 octahedron, with the low-energy singlet always occupied, a double degeneracy remains for the other electron. The orbital degrees of freedom in V^{3+} ion is thus described by an Ising-like variable.

Recent experimental studies on CaV_2O_4 seem to rule out a possible chiral liquid phase as well. A structural transition at $T_s \approx 141$ K reduces the crystal symmetry to monoclinic $P2_1/n$.[8,9] It was suggested in Ref. 8 that the simultaneous orbital ordering relieves the magnetic frustration of zigzag chains. As the interchain frustration is also lifted by the lattice distortion, a three-dimensional Néel order sets in at $T_N \approx 71$ K. The collinear spins are parallel to the crystal b axis as evidenced by both nuclear magnetic resonance and neutron-diffraction measurements.[6–8]

To make progress toward an understanding of the ground-state structure and the nature of phase transitions in CaV_2O_4, here we study the zero-temperature phase diagram of its building blocks, i.e., zigzag chains with $S=1$ spins and Ising orbital variables. We propose a theoretical model which includes the superexchange (SE) interaction, relativistic spin-orbit (SO) coupling, and JT effect. We find that antiferro-orbital order favored by an Ising-like orbital exchange is destroyed in the presence of large on-site spin-orbit or Jahn-Teller coupling. Depending on the underlying orbital configuration, magnetic properties of the zigzag chain are equivalent either to those of two weakly coupled $S=1$ chains or to those of an unfrustrated spin-1 ladder. In the limit of large spin-orbit coupling, the zigzag chain can be viewed as

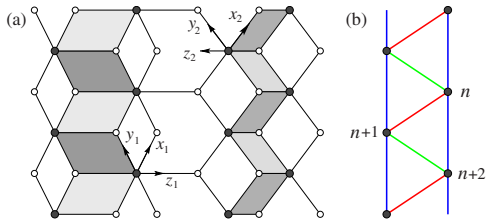

FIG. 1. (Color online) (a) Two crystallographically inequivalent vanadium chains in CaV_2O_4. The V^{3+} ions are arranged in zigzag chains of edge-sharing VO_6 octahedra. For both vanadium sites, the VO_6 octahedra are flattened at room temperatures. A local reference frame is defined in such a way that the z axis is parallel to the tetragonal axis of the crystal field. The black and white circles denote the vanadium and oxygen ions, respectively. (b) A simplified view of the zigzag chain. The red (dark gray), green (light gray), and blue (gray) bonds are parallel to the local [011], [101], and [110] axes, respectively. Consequently, electron hopping on the red (dark gray), green (light gray), and blue (gray) bonds is possible only when d_{yz}, d_{zx}, and d_{xy} orbitals are occupied, respectively.

a spin-2 chain with anisotropic interaction. Finally, we discuss implications for CaV_2O_4.

Model Hamiltonian. We first define a local reference frame for the two crystallographically inequivalent vanadium chains (referred to as type-I and -II chains here) in CaV_2O_4 such that the z axis is parallel to the tetragonal direction of flattened VO_6 octahedron [Fig. 1(a)]. Nearest-neighbor bonds along the chain are parallel to the local [011] and [101] directions alternatively. In the following, we employ a convention in which even-numbered bonds are along the [011] axis.

Geometrical frustration of the zigzag chain comes from the fact that second-nearest-neighbor bonds parallel to the local [110] axis have a length close to that of nearest-neighbor bonds. In fact, the second-nearest-neighbor interaction is the dominant one as the d_{xy} orbital is occupied at every site due to the flattened VO_6 octahedra. The remaining orbital degeneracy is described by a pseudospin $\frac{1}{2}$ with $\sigma^z=\pm 1$ corresponding to the $|yz\rangle$ and $i|zx\rangle$ states, respectively.

Having introduced the basic notations, we now discuss a minimal model for the spin-orbital chain. Since orbital interaction with a 90° angle between vanadium-oxygen bonds is governed by direct $dd\sigma$ exchange of t_{2g} orbitals, the corresponding spin interaction on a bond depends on whether the relevant orbital is occupied.[12] Essentially, orbitals participate in the superexchange only via orbital projectors $P_{yz/zx}$. Noting that $P_{yz/zx}=(1\pm\sigma^z)/2$, we first define the antiferro-orbital and ferro-orbital bond operators,

$$\mathcal{O}_{n,n+1}=\tfrac{1}{2}(1-\sigma_n^z\sigma_{n+1}^z),\quad \overline{\mathcal{O}}_{n,n+1}=\tfrac{1}{4}(1\pm\sigma_n^z)(1\pm\sigma_{n+1}^z),$$

with $\pm$ signs for even- and odd-numbered bonds, respectively. The model Hamiltonian is divided into three parts: $H=H_0+H_\perp+H_{\text{on-site}}$. The first H_0 term represents decoupled spin and orbital systems,

$$H_0=J_2\sum_n \mathbf{S}_n\cdot\mathbf{S}_{n+2}-\sum_n (K\mathcal{O}_{n,n+1}+K'\overline{\mathcal{O}}_{n,n+1}). \quad (1)$$

Since J_2 couples every second-nearest neighbors, the spin part can be viewed as two decoupled $S=1$ Haldane chains, corresponding to the two vertical blue (gray) lines in Fig. 1(b). The K and K' terms denote the energy gain of an antiferro-orbital and a ferro-orbital bond, respectively. In general, we have $K>K'$ due to a finite on-site Hund's coupling J_H, and hence an antiferro-orbital order in the ground state of H_0.

The $H_\perp$ term introduces interactions between the two spin-1 chains,

$$H_\perp=\sum_n (J_1\overline{\mathcal{O}}_{n,n+1}-J_1'\mathcal{O}_{n,n+1})\mathbf{S}_n\cdot\mathbf{S}_{n+1}. \quad (2)$$

As discussed above interaction between spins depends on orbital occupations: the antiferromagnetic coupling J_1 is nonzero only when the d_{yz} (d_{zx}) orbital is occupied at both sites of an even (odd) bond, whereas the strength of ferromagnetic J_1' term depends on the expectation value of the antiferro-orbital bond operator $\mathcal{O}_{n,n+1}$.

Explicit expressions relating the exchange constants to microscopic parameters are obtained from the SE Hamiltonian of vanadium spinels,[12] where neighboring VO_6 octahedra share the same edge as in zigzag chains considered here. Assuming an exact octahedral site symmetry, we find $K=(1+2\eta)(t^2/U)$, $J_2=J_1=K'=(1-\eta)(t^2/U)$, and $J_1'=\eta(t^2/U)$ to lowest order in Hund's parameter $\eta\equiv J_H/U$. Here, t is the hopping integral and U is the on-site Coulomb repulsion. The parameters of the model can be estimated from known values of the same parameters in other vanadium compounds. Measurements on cubic vanadates yield $J_H\simeq 0.68$ eV, $U\simeq 6$ eV, and $t\simeq -0.35$ eV,[13,14] which gives $\eta\simeq 0.11$ and $t^2/U\simeq 20.4$ meV. The estimate of λ is less certain; we find $\lambda\simeq 13-25$ meV.[5,13,15,16] In the following, we shall measure the energy in units of t^2/U.

The remaining single-ion interactions are included in the Hamiltonian

$$H_{\text{on-site}}=-\lambda\sum_n \sigma_n^x S_n^z-\delta\sum_n \sigma_n^z. \quad (3)$$

The first term originates from relativistic SO coupling $\lambda(\mathbf{L}\cdot\mathbf{S})$. Since the d_{xy} orbital is always occupied, the x and y components of the orbital angular momentum are quenched; the remaining $L^z=-\sigma^x$ in the pseudospin representation. A similar situation has been studied in cubic vanadates.[17] The effect of the monoclinic structural transition at T_s is modeled by the second term with 2δ denoting the level splitting due to the induced orthorhombic distortion of VO_6 octahedra. Note that the orthorhombic distortion is different on type-I and -II chains.[8,9]

Orbital orders. We first consider a simpler case of the model Hamiltonian by assuming the presence of a collinear Néel order on the zigzag chain. This is a plausible assumption as the SO term $\lambda\sigma_n^x S_n^z$ breaks the spin SU(2) symmetry and, as will be discussed later, closes the energy gap of longitudinal magnons at large enough λ, hence signaling a transition to the Néel state with S_n^z parallel to $\pm\hat{\mathbf{z}}$. Even with this simplification, the competition between intersite exchange and various on-site interactions still poses a rather nontrivial problem. This study also sheds light on orbital orders in the ground state of CaV_2O_4, where spins develop a three-dimensional collinear antiferromagnetic order at $T_N\approx 71$ K.

Due to the strong second-nearest-neighbor exchange J_2, collinear orders on a zigzag chain consisting of repeated ++−− spins have a quadrupoled unit cell. There are a total of four degenerate Néel states related to each other by lattice translations and time reversal [Figs. 2(a) and 2(b)]. After applying a π rotation about the z axis to pseudospins at $S_n^z<0$ sites, we obtain an effective orbital Hamiltonian,

$$H_{\text{orb}}=\sum_n [\mathcal{J}+(-1)^n\mathcal{K}]\sigma_n^z\sigma_{n+1}^z-\sum_n (h_z\sigma_n^z+h_x\sigma_n^x). \quad (4)$$

This model is equivalent to an Ising chain with alternating nearest-neighbor couplings in a skewed magnetic field. The effective exchange constants are $\mathcal{J}=(2K-K')/4$ and $\mathcal{K}=\nu^2(2J_1'+J_1)/4$. Here, we have assumed $\langle\mathbf{S}_n\cdot\mathbf{S}_{n+1}\rangle=\mp\nu^2$ on even and odd bonds, respectively. The longitudinal and transverse fields are given by $h_z=\delta+\nu^2 J_1/2$ and $h_x=\lambda$, respectively. The parameter $\nu<1$ characterizes the magnitude

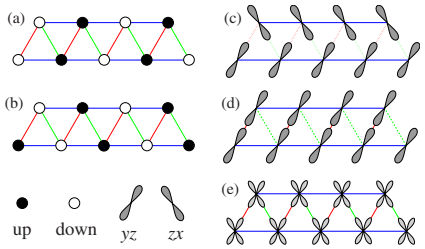

FIG. 2. (Color online) Spin and orbital orders on a zigzag vanadium chain. Néel orders (a) and (b) are related to each other by lattice translations. There are a total of four degenerate Néel states; the other two are related to states (a) and (b) by time reversal. (c) Antiferro-orbital order consisting of staggered d_{yz} and d_{zx} orbitals. (d) and (e) correspond to ferro-orbital orders with real orbital d_{yz} and complex orbitals $(d_{yz} \pm i d_{zx})/\sqrt{2}$, respectively.

of the Néel order. Its value can only be determined with a proper treatment of the SO coupling term. For simplicity, we set $\nu=1$ in the following calculation. Hamiltonian (4) without the staggered exchange $\mathcal{K}$ is one of the simplest models exhibiting nontrivial quantum critical point:[18] numerical calculation shows an order-disorder transition belonging to two-dimensional Ising universality class. The staggered exchange $\mathcal{K}$ involves higher-order spatial derivatives in the continuum limit and thus represents an irrelevant perturbation in the renormalization group (RG) sense.

A schematic phase diagram of model (4) is shown in Fig. 3(a), where an antiferro-orbital phase is separated from the orbital paramagnet by an Ising transition line. Along the δ axis ($\lambda=0$), the antiferro-orbital phase coexists with ferro-orbitally ordered phase, shown in Figs. 2(c) and 2(d), respectively, at the multicritical point $\delta_c=(2K-K'-J_1)/2$. On the other hand, in the large λ limit, the pseudospins are polarized by the transverse field h_x such that spins $S^z=\pm 1$ are accompanied by complex orbitals $\frac{1}{\sqrt{2}}(d_{yz} \pm i d_{zx})$, respectively, resulting in a uniform orbital occupation $n_{yz}=n_{zx}=1/2$ at all sites [Fig. 2(e)]. Using the infinite-system density matrix renormalization group (DMRG) method with periodic boundary condition,[19] we obtain a critical λ_c at $\delta=0$, taking into account the effect of staggered $\mathcal{K}$. The Ising transition line is

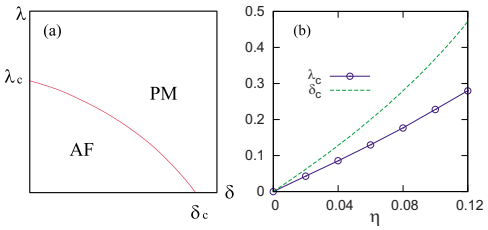

FIG. 3. (Color online) (a) Schematic phase diagram of orbitals in the presence of a collinear Néel order on the zigzag chain, effectively described by Hamiltonian (4). AF and PM refer to antiferro-orbitally ordered and orbital paramagnetic phases, respectively. (b) Critical boundaries λ_c and δ_c measured in units of t^2/U versus Hund's parameter η. The critical distortion is determined analytically from $\delta_c=(2K-K'-J_1)/2$, whereas λ_c is obtained from DMRG calculation. The various effective parameters in Eq. (4) are expressible in terms of model parameters J_1, J_1', J_2, K, and K' of the original SE. Hamiltonian, whose relations to η and t^2/U can be found in the text.

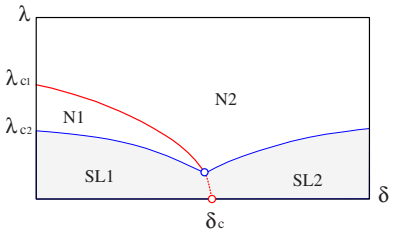

FIG. 4. (Color online) Schematic phase diagram of the zigzag vanadium chain. The various phases are characterized by the magnetic properties. SL and N represent spin-liquid phase and Néel order, respectively. The SL1 and N1 phases are accompanied by an antiferro-orbital order, while in the N2 and SL2 phases the orbitals behave as an orbital paramagnet. The first-order transition along the dashed line is an extension of the multicritical point $(\delta_c,0)$ in the phase diagram in Fig. 3.

bounded by the critical points $(\delta_c,0)$ and $(0,\lambda_c)$. Figure 3(b) shows δ_c and λ_c as functions of the parameter $\eta=J_H/U$. As expected, the antiferro-orbital phase shrinks with decreasing Hund's coupling J_H. In a full quantum treatment of the zigzag chain, we expect a similar critical line characterized by massless orbital excitations (Fig. 4).

Spin-liquid phases. We now discuss the original Hamiltonians (1)–(3) in the small λ limit without assuming the existence of a magnetic order. It is important to note that the spin part of the Hamiltonian in this limit preserves a continuous SU(2) symmetry, which cannot be broken in one dimension. One thus expects stable spin-liquid phases whose properties depend critically on orbital configurations. Furthermore, the absence of σ^x term at $\lambda=0$ indicates that the orbital part is described by a classical Ising-like Hamiltonian. Consequently, the search of ground states reduces to first enumerating over all possible Ising configurations $\{\sigma_n^z\}$ and then comparing their energies taking into account contribution from spins. As antiferro-orbital and ferro-orbital orders are favored by SE and JT interactions, respectively, it is natural to consider these two configurations first.

In the case of antiferro-orbital order [Fig. 2(c)] where bond operators $\langle \bar{\mathcal{O}}_{n,n+1} \rangle = 0$ and $\langle \mathcal{O}_{n,n+1} \rangle = 1$, the zigzag chain behaves as two spin-1 chains weakly coupled by a frustrated ferromagnetic J_1'. The corresponding spin-liquid phase (SL1 phase in Fig. 4) has an energy gap at an incommensurate wave vector.[20] On the other hand, the frustrated J_1' coupling is quenched by the ferro-orbital order shown in Fig. 2(d). Depending on the sign of the ferro-Ising order $\langle \sigma_n^z \rangle = \pm 1$, the J_1 term is nonzero only on even or odd bonds, but not on both. The spin Hamiltonian is equivalent to that of a spin-1 ladder with rung coupling J_1. The magnetic ground state is again disordered (SL2 phase in Fig. 4).[21,22] The magnetic energy of spin-1 ladder with arbitrary rung coupling has been calculated using quantum Monte Carlo method in Ref. 21. Comparing the energy of the two phases, including both spin and orbital contributions, yields a boundary δ_c surprisingly close to the one obtained assuming a Néel order.

Although the SU(2) symmetry is broken in the presence of SO coupling, both spin liquids persist up to finite λ. In the SL2 phase, stable at large JT distortion $\delta > \delta_c$, SO coupling provides an easy-axis anisotropy DS_z^2 with $D \simeq -\lambda^2/2\delta$. The spin-1 ladder undergoes an Ising transition to a Néel phase

(N2 phase in Fig. 4) with increasing λ. At large δ, the condition $D=D_c$ gives rise to a critical $\lambda_c \propto \sqrt{\delta}$. On the other hand, Néel transition at small δ can be understood by considering the λ dependence of the spin gap in SL1 phase. The singlet ground state of weakly coupled Haldane chains has triply degenerate magnon excitations with dispersion $\omega_k = \sqrt{\Delta_0^2 + v^2(k-k_0)^2}$. In the limit of vanishing J_1', the system reduces to two decoupled Haldane chains with $k_0=\pi$, $\Delta_0 = 0.410 J_2$ (Haldane gap for spin 1), and $v = 2.49 J_2$.[23] A simple second-order perturbation calculation adds a correction to the spin gap,

$$\Delta = \Delta_0 - \frac{\lambda^2 |\langle 0|S_n^z|k_0\rangle|^2}{\Delta_\sigma - \Delta_0}, \tag{5}$$

where $\Delta_\sigma \approx 2(\delta_c - \delta)$ is the energy of a domain-wall pair (a flipped pseudospin in the antiferro-orbital state), $|0\rangle$ is the singlet ground state, and $|k\rangle$ denotes one-magnon excitation with wave vector k. The matrix element $\langle 0|S_n^z|k\rangle = \sqrt{Z}e^{ikn}$, with $Z \approx 1$.[23] For $\Delta_\sigma > \Delta_0$, the spin gap decreases with increasing λ and eventually reaches zero at $\lambda_{c2} \propto \sqrt{2(\delta_c - \delta) - \Delta_0}$, signaling a transition into magnetically ordered phase (N1 phase).

The two Néel phases in Fig. 4 are distinguished by the underlying orbital orders; the phase boundary λ_{c1} separating N1 from N2 phases is thus analogous to the Ising transition line of the orbital only model [Fig. 3(b)]. Since the upper critical $\lambda_{c1} \propto J_H$, at small Hund's coupling the zigzag chain could bypass the N1 phase and enter the orbital paramagnetic phase simultaneously with a magnetic ordering. A conjectured phase diagram of the zigzag chain is shown in Fig. 4.

Anisotropic $J=2$ spin chain. In the limit of large SO coupling, the appropriate degrees of freedom are effective spins of length $J=2$, where $\mathbf{J}=\mathbf{L}'+\mathbf{S}$ and $L'=1$ is the angular momentum of the unoccupied t_{2g} hole. The system thus behaves as a spin-2 chain with anisotropic exchange interaction.[5] Furthermore, JT coupling adds an anisotropy $DJ_z^2 + E(J_x^2 - J_y^2)$, where $D<0$ and $E \propto \delta$ are proportional to the tetragonal and orthorhombic distortions of VO_6 octahedron, respectively. Assuming a dominating easy-axis anisotropy $|D| \gg E$, the N2 phase can also be viewed as Néel ordering of the effective spins $J_z = \pm 2$ in such a way that spins of a given direction $S_z = \pm 1$ are coupled to orbital angular momenta $L_z' = \pm 1$, respectively. The corresponding ferro-orbital order with complex orbitals $d_{yz} \pm i d_{zx}$ is shown in Fig. 2(e). The V^{3+} ions have a reduced magnetic moment $\mu = (2S - L')\mu_B = 1\mu_B$.

We have presented and analyzed a minimal model of frustrated vanadium chains, pertinent to quasi-1D compound CaV_2O_4. A conjectured phase diagram (Fig. 4) is obtained based on analytical arguments and numerical calculations. The observed $P2_1/n$ crystal symmetry of CaV_2O_4 at low temperatures indicates that only *two* inequivalent vanadium sites exist as in the high-temperature phase. The absence of doubled unit cell resulting from antiferro-orbital order thus implies that both vanadium chains are in the orbital paramagnetic phase. This is a plausible conclusion noting that a rather small $\lambda_{c1} \approx 0.22(t^2/U) \approx 4.5$ meV is estimated from Fig. 3 assuming $\eta \approx 0.11$. However, the monoclinic distortion below T_s places the two types of vanadium chain at rather distinct regions of the phase diagram.

The type-I chain acquires a small δ in addition to the dominating tetragonal crystal field and behaves as a spin-2 chain subject to an easy-axis anisotropy. This Ising anisotropy is important to the stabilization of three-dimensional Néel order in CaV_2O_4, as the collinear spins are found to point along the easy axis of type-I chains.[8] The measured V moment of $1.06\mu_B$ is also consistent with the picture of an anisotropic spin-2 chain.[7] On the other hand, a strong orthorhombic distortion δ at type-II ions completely removes the orbital degeneracy and makes the vanadium chains effectively spin-1 ladders. In fact, the well-separated t_{2g} levels at type-II ions lead to a possible easy-plane spin anisotropy.[8] Consequently, induced collinear order on type-II chains follows the spin direction of type-I vanadium ions, as indeed observed in CaV_2O_4.

We acknowledge fruitful discussions with A. Chubukov, D. Johnston, G. Japaridze, O. Kolezhuk, B. Lake, O. Pieper, and O. Tchernyshyov.

[1] M. Imada, A. Fujimori, and Y. Tokura, Rev. Mod. Phys. **70**, 1039 (1998).
[2] S.-H. Lee *et al.*, Phys. Rev. Lett. **93**, 156407 (2004).
[3] V. O. Garlea, R. Jin, D. Mandrus, B. Roessli, Q. Huang, M. Miller, A. J. Schultz, and S. E. Nagler, Phys. Rev. Lett. **100**, 066404 (2008).
[4] H. Tsunetsugu and Y. Motome, Phys. Rev. B **68**, 060405(R) (2003).
[5] O. Tchernyshyov, Phys. Rev. Lett. **93**, 157206 (2004).
[6] J. Hastings *et al.*, J. Phys. Chem. Solids **28**, 1089 (1967).
[7] X. Zong, B. J. Suh, A. Niazi, J. Q. Yan, D. L. Schlagel, T. A. Lograsso, and D. C. Johnston, Phys. Rev. B **77**, 014412 (2008).
[8] O. Pieper *et al.*, Phys. Rev. B **79**, 180409(R) (2009).
[9] A. Niazi *et al.*, Phys. Rev. B **79**, 104432 (2009).
[10] H. Kikuchi, M. Chiba, and T. Kubo, Can. J. Phys. **79**, 1551 (2001).
[11] T. Hikihara *et al.*, J. Phys. Soc. Jpn. **69**, 259 (2000).
[12] S. Di Matteo, G. Jackeli, and N. B. Perkins, Phys. Rev. B **72**, 020408(R) (2005).
[13] T. Mizokawa and A. Fujimori, Phys. Rev. B **54**, 5368 (1996).
[14] K. Takubo, J. Y. Son, T. Mizokawa, H. Ueda, M. Isobe, Y. Matsushita, and Y. Ueda, Phys. Rev. B **74**, 155103 (2006).
[15] A. Abragam and B. Bleaney, *Introduction to Ligand Field Theory* (Clarendon Press, Oxford, 1970), pp. 377–378; A. Abragam and B. Bleaney, *ibid.*, pp. 426–429.
[16] A. Tanaka, J. Phys. Soc. Jpn. **71**, 1091 (2002).
[17] P. Horsch, G. Khaliullin, and A. M. Oleś, Phys. Rev. Lett. **91**, 257203 (2003).
[18] A. A. Ovchinnikov, D. V. Dmitriev, V. Ya. Krivnov, and V. O. Cheranovskii, Phys. Rev. B **68**, 214406 (2003).
[19] S. R. White, Phys. Rev. B **48**, 10345 (1993).
[20] D. Allen and D. Sénéchal, Phys. Rev. B **61**, 12134 (2000).
[21] D. Sénéchal, Phys. Rev. B **52**, 15319 (1995).
[22] S. Todo, M. Matsumoto, C. Yasuda, and H. Takayama, Phys. Rev. B **64**, 224412 (2001).
[23] I. Affleck and R. A. Weston, Phys. Rev. B **45**, 4667 (1992).